Regulation of the thermoalkaliphilic F_1-ATPase from *Caldalkalibacillus thermarum*

Scott A. Ferguson[a], Gregory M. Cook[a,b], Martin G. Montgomery[a], Andrew G. W. Leslie[c], and John E. Walker[a,1]

[a]Medical Research Council Mitochondrial Biology Unit, Cambridge Biomedical Campus, Cambridge CB2 0XY, United Kingdom; [b]Department of Microbiology and Immunology, University of Otago, Dunedin 9016, New Zealand; and [c]Medical Research Council Laboratory of Molecular Biology, Cambridge Biomedical Campus, Cambridge CB2 0QH, United Kingdom

Contributed by John E. Walker, July 25, 2016 (sent for review June 19, 2016; reviewed by Thomas M. Duncan and Dale B. Wigley)

The crystal structure has been determined of the F_1-catalytic domain of the F-ATPase from *Caldalkalibacillus thermarum*, which hydrolyzes adenosine triphosphate (ATP) poorly. It is very similar to those of active mitochondrial and bacterial F_1-ATPases. In the F-ATPase from *Geobacillus stearothermophilus*, conformational changes in the ε-subunit are influenced by intracellular ATP concentration and membrane potential. When ATP is plentiful, the ε-subunit assumes a "down" state, with an ATP molecule bound to its two C-terminal α-helices; when ATP is scarce, the α-helices are proposed to inhibit ATP hydrolysis by assuming an "up" state, where the α-helices, devoid of ATP, enter the $\alpha_3\beta_3$-catalytic region. However, in the *Escherichia coli* enzyme, there is no evidence that such ATP binding to the ε-subunit is mechanistically important for modulating the enzyme's hydrolytic activity. In the structure of the F_1-ATPase from *C. thermarum*, ATP and a magnesium ion are bound to the α-helices in the down state. In a form with a mutated ε-subunit unable to bind ATP, the enzyme remains inactive and the ε-subunit is down. Therefore, neither the γ-subunit nor the regulatory ATP bound to the ε-subunit is involved in the inhibitory mechanism of this particular enzyme. The structure of the $\alpha_3\beta_3$-catalytic domain is likewise closely similar to those of active F_1-ATPases. However, although the β_E-catalytic site is in the usual "open" conformation, it is occupied by the unique combination of an ADP molecule with no magnesium ion and a phosphate ion. These bound hydrolytic products are likely to be the basis of inhibition of ATP hydrolysis.

Caldalkalibacillus thermarum | F_1-ATPase | structure | inhibition | regulation

The F-ATPases (F_1F_o-ATP synthases) from chloroplasts, mitochondria, and eubacteria have evolved different ways of regulating ATP hydrolysis (1). During darkness, chloroplast F-ATPases use a redox inhibitory mechanism (2, 3). Mitochondrial enzymes bind an inhibitor protein called IF_1, inhibitor of F_1-ATPase (4–7), and α-proteobacterial F-ATPases have a related inhibitor protein called the ζ-subunit (8–10). Many eubacterial F-ATPases synthesize ATP in the presence of oxygen and, under anaerobic conditions, hydrolyze ATP made by substrate-level phosphorylation to generate the proton-motive force, which is required for maintaining cell viability in the absence of growth. When the proton-motive force and cellular ATP concentration are low, an inhibitory mechanism that may operate to prevent ATP wastage has been demonstrated in vitro for the F-ATPases from *Escherichia coli* (11), *Geobacillus stearothermophilus* (12), and *Thermosynechococcus elongatus* (13) involving their ε-subunit. This subunit, a component of the rotor of the enzyme, is folded into an N-terminal nine-stranded β-sandwich and a C-terminal α-helical hairpin (13–18). The β-sandwich binds the subunit to the γ-subunit and to the c ring in the membrane domain, and the α-helices adopt two conformations, "down" and "up." In the down state of the F-ATPase from *G. stearothermophilus*, the α-helices of the ε-subunit bind an ATP molecule and are associated with the β-sandwich (17); in the absence of bound ATP, the α-helices assume the up position, interacting with the $\alpha_3\beta_3$-domain and inhibiting ATP hydrolysis (18). Up positions have been captured in structures of the F_1-domains from *E. coli* (19, 20), but the isolated ε-subunit remains in a down conformation even when ATP is not bound to it (14–16). Deletion of its five C-terminal amino acids diminished respiratory growth (21), but deletion of the C-terminal domain had no growth phenotype (22).

The F-ATPases from the thermoalkaliphile *Caldalkalibacillus thermarum* (23) from mycobacterial species (24, 25) and from alkaliphilic *Bacilli* (26, 27) exemplify classes of eubacterial enzymes with F-ATPases that can synthesize ATP but show extreme latency in hydrolyzing ATP, although a weak ATPase activity can be stimulated artificially in vitro (23–27). The modes of inhibition of the hydrolytic activity is not understood, although it has been suggested that the *C. thermarum* enzyme is inhibited by the γ-subunit having adopted a modified structure (28). The γ-subunit is a key component of the enzyme's rotor.

As described here, we have investigated possible mechanisms of inhibition of the F_1-ATPase from *C. thermarum* by studying the structure and properties of a version lacking the δ-subunit (referred to as F_1-ATPase); the δ-subunit is part of the enzyme's stator, and has no direct role in the mechanism or regulation of ATP hydrolysis. We have reinvestigated the proposal that, in the inhibited enzyme, the γ-subunit has a modified structure, and have studied a form of the enzyme with two mutations in a region of the ε-subunit where the proposed regulatory ATP molecule is bound in *E. coli* and *G. stearothermophilus* (17, 29). Our study shows that neither the γ-subunit nor the regulatory ATP bound to the

Significance

Adenosine triphosphate (ATP), the fuel of life, is produced by a molecular machine consisting of two motors linked by a rotor. One generates rotation by consuming energy derived from oxidative metabolism or photosynthesis; the other uses energy transmitted by the rotor to put ATP molecules together from their building blocks adenosine diphosphate and phosphate. In many species the machine is easily reversible, and various different mechanisms to regulate the reverse action have evolved so that it is used only when needed. In some eubacterial species, including the thermoalkaliphile *Caldalkalibacillus thermarum*, although evidently constructed in a similar way to reversible machines, the reverse action is severely impeded, evidently because the products of hydrolysis remain bound to the machine.

Author contributions: J.E.W. designed research; J.E.W. supervised the project; S.A.F., G.M.C., and M.G.M. performed research; S.A.F., G.M.C., M.G.M., A.G.W.L., and J.E.W. analyzed data; and M.G.M. and J.E.W. wrote the paper.

Reviewers: T.M.D., State University of New York Upstate Medical University; and D.B.W., Imperial College London.

The authors declare no conflict of interest.

Freely available online through the PNAS open access option.

Data deposition: The crystallography, atomic coordinates, and structure factors reported in this paper have been deposited in the Protein Data Bank, www.pdb.org (PDB ID codes 5HKK and 5IK2).

[1]To whom correspondence should be addressed. Email: walker@mrc-mbu.cam.ac.uk.

This article contains supporting information online at www.pnas.org/lookup/suppl/doi:10.1073/pnas.1612035113/-/DCSupplemental.

ε-subunit is involved in the inhibitory mechanism, and that probably ATP hydrolysis is prevented by hydrolysis products bound to a catalytic subunit.

Results

Structure Determination. The purified wild-type and mutant F_1-ATPases from *C. thermarum* consist of the α-, β-, γ-, and ε-subunits (Fig. S1). The ATP hydrolysis activity of the wild-type and mutant F_1-complexes was activated by lauryldimethylamine oxide [LDAO; 0.1% (vol/vol)] to a specific activity of 33–38 U/mg protein for both enzymes. The crystal structure of the wild-type enzyme (Fig. 1 *A* and *B*) was solved by molecular replacement with data to 3.0-Å resolution. The asymmetric unit contains two copies of the complex. The electron density for one copy was slightly better than for the other, but their structures are very similar, with an rmsd in main-chain atoms of 0.37 Å. Data processing and refinement statistics for both structures are summarized in Table S1. The final model of the better-defined copy of the wild-type complex (complex 1) contains the following residues: α_E, 26–500; α_{TP}, 27–501; α_{DP}, 27–502; β_E, 2–462; β_{TP}, 2–462; β_{DP}, 2462; γ, 3–286; and ε, 3–134. The second copy (complex 2) contains α_E, 27–500; α_{TP}, 27–501; α_{DP}, 25–502; β_E, 2–462; β_{TP}, 2–462; β_{DP}, 2–462; γ, 3–286; and ε, 3–134. In both structures, the nucleotide binding sites in the β_{DP}- and β_{TP}-subunits and in the three α-subunits are occupied by Mg-ADP. The β_E-subunit contains ADP, without an accompanying magnesium ion, at 50–75% occupancy, plus density interpreted as a phosphate ion at an occupancy of 100% (Fig. S2). An ATP molecule with a magnesium ion is bound in the C-terminal α-helical domain of the ε-subunit.

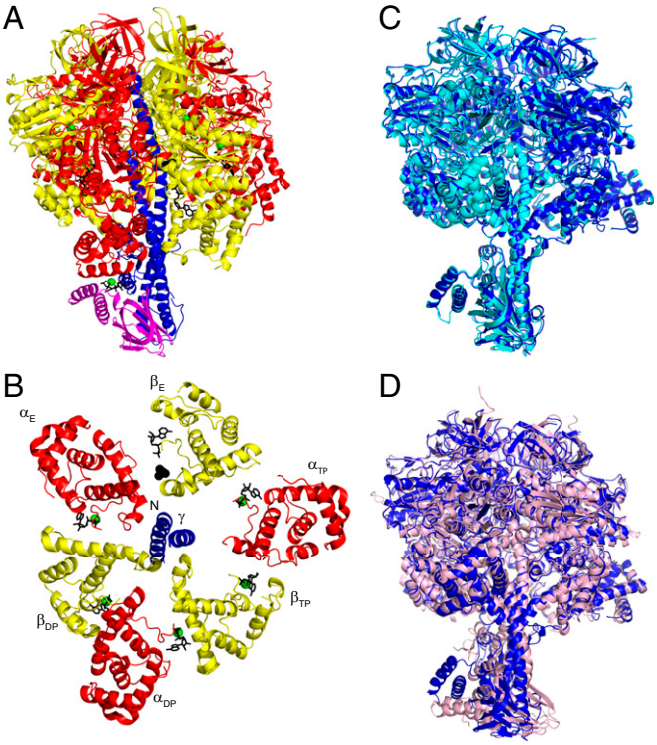

Fig. 1. Structure of the F_1-ATPase from *C. thermarum*. (*A*) Side view of the wild-type structure in ribbon representation with the α-, β-, γ-, and ε-subunits in red, yellow, blue, and magenta, respectively, and bound nucleotides in black. (*B*) Cross-sectional view of the C-terminal domains of the α- and β-subunits, upward from the foot of the central stalk along the axis of the γ-subunit, showing the occupancy of nucleotides in nucleotide-binding domains. Green spheres represent magnesium ions, and black spheres denote a phosphate ion bound to the β_E-subunit. (*C*) Comparison of the wild-type and mutant complexes, in blue and cyan, respectively; the structures are superimposed via their $\alpha_3\beta_3$-domains. (*D*) Comparison of structures of F_1-ATPases from *C. thermarum* (blue) and bovine mitochondria (pink).

The mutant F_1-ATPase complex from *C. thermarum* was solved by molecular replacement using the $\alpha_3\beta_3$-domain from the wild-type structure with data to 2.6-Å resolution (Table S1). Like the wild-type structure, the asymmetric unit of the mutant enzyme contains two copies of the complex, complexes 1 and 2, with electron densities of similar quality. The model of complex 1 contains residues α_E, 27–501; α_{TP}, 26–395, 403–501; α_{DP}, 26–398, 401–502; β_E, 1–462; β_{TP}, 1–462; β_{DP}, 2–462; γ, 2–286; and ε, 3–134. The resolved regions of complex 2 are almost identical, and the model contains the following residues: α_E, 27–501; α_{TP}, 26–394, 403–501; α_{DP}, 24–399, 403–502; β_E, 1–462; β_{TP}, 1–462; β_{DP}, 1–462; γ, 2–286; and ε, 1–134. The occupancy of nucleotides in the α- and β-subunits was the same as in the wild-type structure, with full occupancy of the ADP in the β_E-subunit. Water molecules were built into the mutant structure but, because of its relatively modest resolution, only in some instances in the wild-type structure. The wild-type and mutant structures resemble each other closely, and the rmsd value of all atoms of the superimposed structures (Fig. 1*C*) is 0.91 Å. The higher resolution of the mutant structure revealed that the magnesium ions associated with ADP molecules in the β_{TP}- and β_{DP}-catalytic sites are hexacoordinated by four water molecules, the hydroxyl group of βThr158, and the oxygen atom O2B of the adenosine, as in structures of mitochondrial F_1-ATPases (5–7, 30–34). Also, in the nucleotide-binding domains of the β_E-subunits, there was additional density interpreted as a phosphate ion. The only significant difference between the wild-type and mutant structures is that an ATP molecule and an accompanying magnesium ion are bound to the ε-subunit of the former but not the latter. Currently, the structure of the mutant F_1-ATPase from *C. thermarum* is the highest-resolution structure of a bacterial F_1-ATPase to have been described, and it represents a significant contribution toward establishing a high-resolution molecular structure of an intact bacterial F-ATPase.

The γ-Subunit. The γ-subunit of the F_1-ATPase from the *C. thermarum* enzyme is folded into two α-helices in its N- and C-terminal regions (residues 1–59 and 210–286, respectively), with an intervening Rossmann fold (residues 76–189). The Rossmann fold has five β-strands with α-helices between strands 1 and 2, 2 and 3, and 3 and 4. The N- and C-terminal α-helices form an antiparallel coiled-coil that lies along the central axis of the $\alpha_3\beta_3$-domain, with the extreme C-terminal region occupying the central cavity of the annular "crown." This coiled-coil extends below the $\alpha_3\beta_3$-domain, where it is associated with the Rossmann-fold domain and with the nine-stranded β-structure of the N-terminal domain of the ε-subunit.

The structure of the γ-subunit of the F_1-ATPase from *C. thermarum* resembles closely those described previously in the structures of F_1-ATPases from eubacteria and mitochondria, as expected from the conservation of sequences, especially in the C-terminal region (Fig. S3). In the structure it occupies a central position, as in other F_1-ATPases. It is most closely related to the γ-subunits from *E. coli* (19), *G. stearothermophilus* (18), and *Paracoccus denitrificans* (10), which have almost exactly the same fold (Fig. 2 *A*–*C*). It is also similar to the γ-subunit in the bovine enzyme (Fig. 2*D*), but the α-helices in the coiled-coil of the bovine protein deviate from the pathway of the bacterial coiled-coil in the lower region, and the foot of the γ-subunit in *C. thermarum* is rotated by about 15° counterclockwise as viewed from the membrane domain of the enzyme relative to the γ-subunit in a structure of bovine F_1-ATPase, where the γ- and ε-subunits are fully resolved (30). As a consequence, in the superimposed structures (Fig. 2*D*) the Rossmann folds are displaced relative to each other.

In contrast to the likeness between the structures of the γ-subunits in bacterial and mitochondrial F_1-ATPases, including

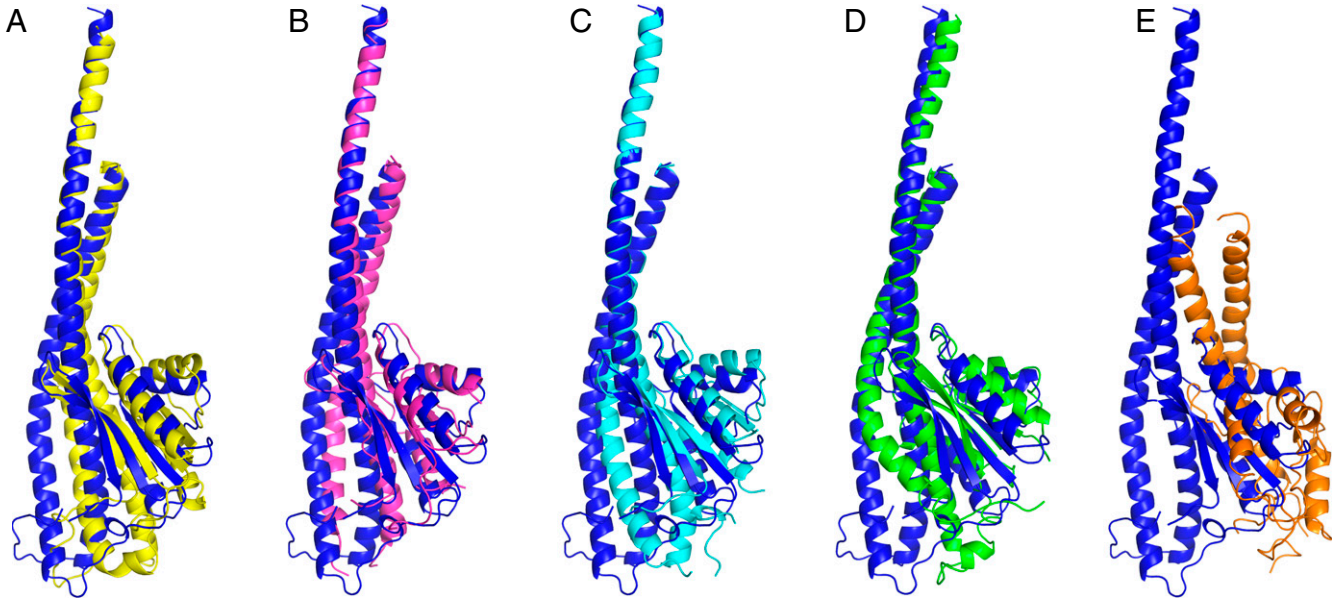

Fig. 2. Comparison of the structures of γ-subunits of the F_1-ATPases in eubacteria and mitochondria. The structures shown from the side in each panel have been abstracted from the pairwise comparisons made by superimposition of the crown domain of structures of F_1-ATPases. The following pairwise comparisons of γ-subunits are shown: *C. thermarum* from the wild-type structure in the current work (blue) versus (*A*) *E. coli* (yellow; residues 1–264), (*B*) *G. stearothermophilus* (pink; residues 2–58, 69–104,106–130, 133–162, 164–192, and 209–284), (*C*) *P. denitrificans* (light blue; residues 13–62, 64–73, 78–110, 115–143, 147–166, 170–199, and 212–289), (*D*) bovine mitochondria (green; residues 1–61, 67–96, and 101–272), and (*E*) *C. thermarum* from a structure of nucleotide-free F_1-ATPase (orange; residues 3–49, 64–193, and 217–266).

that of *C. thermarum* determined in the present work, in a published structure of the nucleotide-free F_1-ATPase from *C. thermarum* (28) the γ-subunit is radically different. In this earlier structure, the α-helical coiled-coil (residues 3–49 and 217–266) is displaced from the central axis of the $\alpha_3\beta_3$-domain toward the β-subunits by ∼20°, and the C-terminal α-helix is truncated by disorder in its C-terminal region. It has three additional α-helical segments from residues 89–101, 119–128, and 149–161, with loops from residues 64–88, 102–188, 129–148, and 162–193. Residues 1–2, 50–63, and 194–216 were unresolved. The α-helices from residues 89–101 and 119–128 correspond to α-helices 1 and 2 in the Rossmann fold of the current structures, respectively. The many differences between this earlier structure and the current one are illustrated in Fig. 2*E*.

The ε-Subunit. In the structure of the wild-type F_1-ATPase from *C. thermarum*, the ε-subunit is in the down position with an ATP molecule bound to it. Therefore, because the enzyme is already inhibited, this mechanism of inhibition of ATP hydrolysis cannot involve the ε-subunit assuming the up position in the absence of a bound ATP molecule. The finding that the removal of the capacity of the ε-subunit to bind ATP has no effect on the inhibition of the enzyme additionally removes any possibility that the bound ATP molecule could be involved in some other unspecified inhibitory mechanism. The structures of the wild-type and mutant forms of the ε-subunit are essentially identical (rmsd for Cα-atoms 0.50 Å). In both forms, the N-terminal region (residues 3–84) has nine β-strands arranged in a β-sandwich, followed by two α-helices (residues 90–106 and 113–132) in a hairpin lying alongside the N-terminal domain. As shown in Fig. 3, they are both similar to the structures of the ε-subunit from *G. stearothermophilus* (rmsd for Cα-atoms 1.79 Å) (17), *E. coli* (rmsd 1.67 Å) (15), *T. elongatus* (rmsd 2.20 Å) (13), and *P. denitrificans* (N-terminal domain only; rmsd 1.12 Å) and to the δ-subunit of F_1-ATPase from bovine mitochondria (rmsd 3.27 Å) (30).

The only significant difference between the mutant and wild-type structures of the ε-subunit from *C. thermarum* is that an ATP molecule and an accompanying magnesium ion are bound by the two α-helices in the wild-type ε-subunit but not in the mutant form. This bound ATP has an unusual compact structure, bent by about 60° at the α-phosphate relative to the conformation, for example, of an ATP molecule bound to the β_{DP}-subunit of the F_1-ATPase from *P. denitrificans* (10) (Fig. S4). This conformation is characteristic of regulatory ATP molecules, whereas substrate ATP molecules are extended (35). The bound ATP is accompanied by a magnesium ion, and the O2A and O2B atoms of the ATP molecule provide two of the six ligands; the other four are almost certainly unresolved water molecules. As expected (17), both Asp89 and Arg92 help to stabilize the bound ATP. The backbone oxygen and nitrogen atoms of Asp89 interact with the adenine ring, and the side chain of Arg92 stacks on top of the adenine ring with the guanidino moiety involved in π–π interactions (Fig. 3 *B* and *C*). Residues Glu83, Ile88, and Ala93 also contribute to the adenine-binding pocket. Residue Arg92 interacts additionally with the ribose and the γ-phosphate, and residues Arg99, Arg123, and Arg127 help to coordinate the phosphates.

The ε-subunit from *C. thermarum* is also closely related to its mitochondrial ortholog, the δ-subunit of their F-ATPases (Fig. S5). The somewhat elevated rmsd value for Cα-atoms of 3.27 Å with the bovine δ-subunit (30) reflects the slight difference in the curvature of the β-strands in the bacterial and mitochondrial orthologs (Fig. 3*D*). However, in structures of F_1-ATPases from bovine and yeast mitochondria, an ATP molecule is not bound to the δ-subunit. Rather, the binding site in mitochondrial δ-proteins has evolved to bind the ε-subunit (which has no eubacterial equivalent). From residues 10–25 the 50-residue bovine ε-subunit is folded into a single α-helix, bound in a groove between the two domains of the bovine δ-subunit, where it occludes the pocket occupied by ATP in the bacterial ε-subunit (Fig. 3*D*).

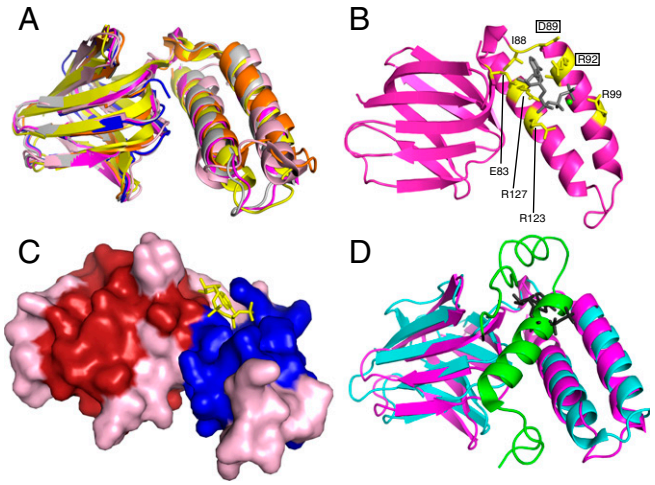

Fig. 3. Comparison of structures of ε-subunits of F-ATPases. (*A*) Superimposed structures of ε-subunits from *C. thermarum* (magenta, wild-type; gray, mutant), *G. stearothermophilus* (orange), *E. coli* (yellow), *P. denitrificans* (β-sheet domain; blue), and *T. elongatus* (pink). (*B*) The ATP binding site in the ε-subunit of the wild-type enzyme. ATP (gray) is bound to a magnesium ion (green sphere) next to C-terminal α-helices 1 and 2 of the ε-subunit (magenta). Residues Glu83, Ile88, Asp89, Arg92, Arg99, Arg123, and Arg127 (yellow) contribute to the binding site; the boxed residues were changed to alanine in the mutant form. (*C*) The ε-subunit in *C. thermarum* illustrating the surface binding site for ATP. The N-terminal β-domain and C-terminal α-helices are red and blue, respectively, and connecting loops are pink; the bound ATP molecule is yellow. (*D*) Superimposition of the *C. thermarum* ε-subunit (magenta) with ATP bound (black), and the bovine δ-subunit (cyan) bound to its cognate ε-subunit (green).

The $\alpha_3\beta_3$-Domain. In both mutant and wild-type forms of the enzyme from *C. thermarum*, the F_1-ATPase and the $\alpha_3\beta_3$-domain are asymmetrical, with similar architectures to the enzymes from bovine and yeast mitochondria. Their close similarity is demonstrated by the superimposition of their structures (Fig. 1*D*). The rmsd values for the Cα-atoms are 5.57 and 2.71 Å, respectively, for the F_1-ATPases and 1.28 and 1.24 Å for the corresponding $\alpha_3\beta_3$-domains.

A striking feature of both the wild-type and mutant structures of the *C. thermarum* F_1-ATPase is that the catalytic site of the β_E-subunit contains an ADP molecule without an associated magnesium ion, and also additional electron density interpreted as a phosphate ion (Fig. 4 *A* and *B*). As in other structures of F_1-ATPase, the adenine moiety is bound in a pocket provided by the side chains of residues Tyr345 and Phe424, and the diphosphate part of ADP is associated with the P-loop sequence, which is Gly-Ala-Gly-Val-Gly-Lys-Thr (residues 152–158) in *C. thermarum*. The side chain of the "arginine finger" residue α-Arg365 (equivalent to bovine α-Arg373) (Fig. 4 *C*–*F*), an essential component of the catalytic mechanism, also points toward the bound phosphate, although there is evidence of an alternate conformation, as in the ground-state structure of the bovine F_1-ATPase (Fig. 4*F*). The phosphate-binding pocket contains residues Lys157, Arg184, Asp245, Asn246, and Arg249, with their side chains interacting with the oxygen atoms of the phosphate, as usual. The phosphate itself is about 7 Å from where the γ-phosphate of an ATP molecule would be if bound to a β_E-subunit. The corresponding electron density was interpreted as phosphate rather than sulfate, as the enzyme had not been exposed to any oxyanions. The purification buffers included 1 mM Mg-ADP but the crystallization buffers were devoid of nucleotide, and therefore it is likely that both the bound ADP and the phosphate originated in the *E. coli* strain used to overexpress the enzymes.

The presence of both a bound ADP molecule (lacking an accompanying magnesium ion) and a bound phosphate ion in the β_E-subunit of an F_1-ATPase is unique among reported structures of the enzyme. In structures of bovine F_1-ATPase, the β_E-subunit is occupied by an ADP molecule, and no magnesium ion, when crystals were grown in the presence of the magnesium chelator phosphonate (33) (Fig. 4*C*), and the phosphate analog thiophosphate (34) occupies a similar position to the phosphate in the current structures (Fig. 4*D*). Phosphate has been found also in a similar position in structures of yeast F_1-ATPase (36), the bovine F_1–c_8 ring complex (37) (Fig. 4*E*), and bovine F_1-ATPase inhibited with dicyclohexylcarbodiimide (30). In the ground-state structure of bovine F_1-ATPase determined at 1.9-Å resolution (38), neither nucleotide nor phosphate occupied the β_E-subunit (Fig. 4*F*).

Discussion

The proposal that the ATP hydrolase activity of the F_1-ATPase from *C. thermarum* is inhibited by the γ-subunit adopting an extensively modified structure (28) has been reexamined. In the inhibited complex, the γ-subunit has a structure closely resembling those of γ-subunits in catalytically active F_1-ATPases from other bacterial and mitochondrial sources. It is unlikely that the differences can be attributed to the earlier structure of enzyme from *C. thermarum* being made with enzyme devoid of bound nucleotides (28) because in a structure of the F_1-ATPase from *Saccharomyces cerevisiae*, also determined with no bound nucleotides (39), the structure of the γ-subunit is very similar (rmsd 1.12 Å) to that determined when bound nucleotides were present in the same enzyme (36). Therefore, there is no good structural reason to invoke the remodeling of the γ-subunit as the inhibitory mechanism. In addition, the structure of the $\alpha_3\beta_3$-domain and the penetrant region of the γ-subunit, which lies along its central axis, do not differ in any discernible way from those of active F_1-ATPases. Therefore, the basis of the inhibitory mechanism is probably associated with some other features of the enzyme.

One possibility that has been considered is that the ε-subunit may contribute to this inhibitory mechanism as reported in other bacterial F-ATPases (11–13, 17–21). In the active F_1-ATPase from *G. stearothermophilus*, for example, the ε-subunit has been observed in the down position with the C-terminal α-helical hairpin, and bound ATP, alongside the N-terminal β-domain (17). It has been proposed that when the proton-motive force and ATP concentration are low, the ATP molecule leaves the ε-subunit, allowing its two α-helices to dissociate from the β-domain, forming the inhibitory up conformation (17–20, 40). In this conformation, the α-helices penetrate into the catalytic domain along the axis of the coiled-coil in the γ-subunit. In the structure of the inhibited wild-type F_1-ATPase from *C. thermarum* the ε-subunit is down, with an ATP molecule bound to it. Therefore, to test the possibility that the ATP molecule bound to the ε-subunit plays some hitherto unconsidered role in inhibiting the *C. thermarum* F_1-ATPase, the ATP-binding capacity was removed by mutation. The enzyme remained inactive, and the structure of the ε-subunit was unchanged with its C-terminal α-helices still down. Therefore, it is unlikely that the ε-subunit, and its bound ATP molecule, contributes to this inhibitory mechanism.

A characteristic feature of bacterial F-ATPases with latent hydrolytic activity is that ATP hydrolysis can be activated artificially in vitro (26, 27) and, for example, LDAO activates the *C. thermarum* F_1-ATPase (41). Removal of the C-terminal domain of the ε-subunit activated the enzyme partially (41), and LDAO activated this mutated enzyme to its fullest extent. LDAO also stimulates the activities of F_1-ATPases that can hydrolyze ATP, by releasing ADP from a catalytic site (42, 43). Thus, it is possible that in vitro activation of the *C. thermarum* F_1-ATPase with LDAO (41) may proceed by a combination of perturbation of the interaction between the ε-subunit and $\alpha_3\beta_3$-domain (41, 44, 45) and an effect on one or more catalytic sites.

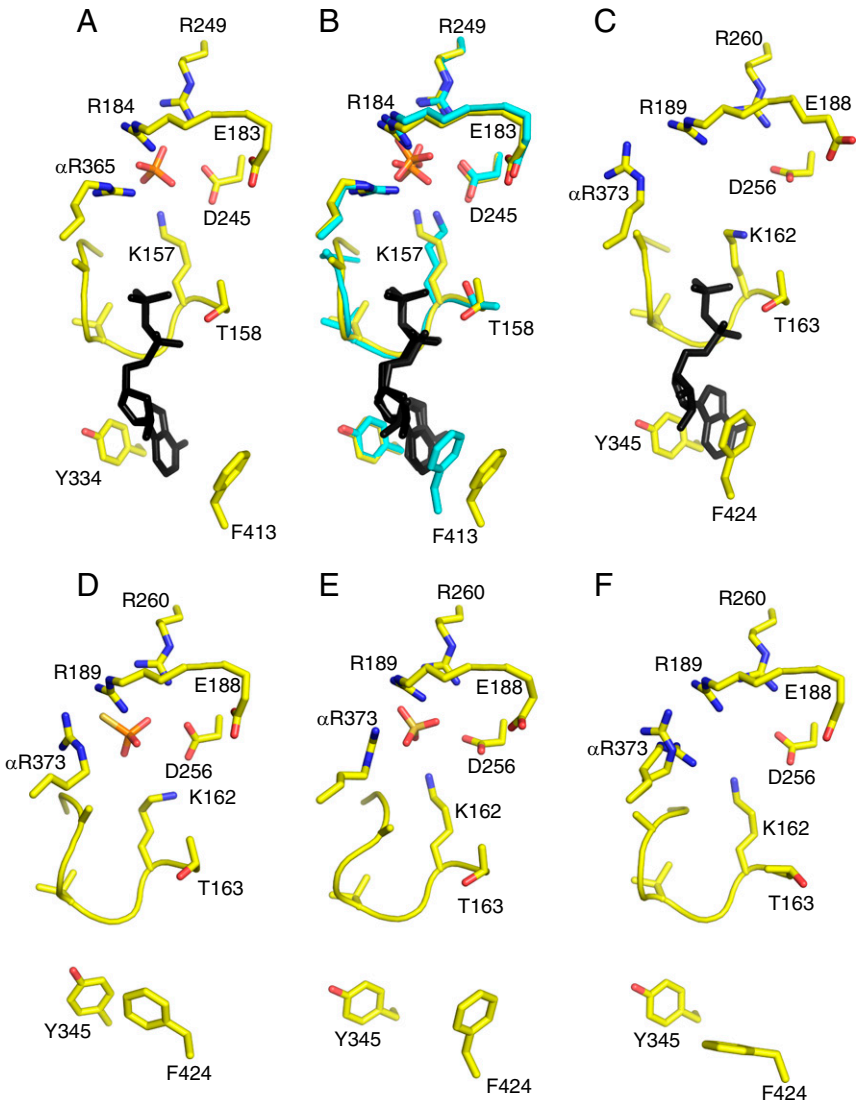

Fig. 4. Comparison of the β_E-catalytic site in the F_1-ATPase from *C. thermarum* with those in various structures of bovine F_1-ATPase. (*A*) The β_E-catalytic site in the wild-type enzyme from *C. thermarum*. (*B*) Comparison of the β_E-catalytic sites in the wild-type (yellow) and mutant (blue) forms of the enzyme from *C. thermarum*. (*C* and *D*) The β_E-catalytic sites in bovine F_1-ATPase crystallized in the presence of phosphonate (*C*) and thiophosphate (*D*). (*E*) The complex of bovine F_1-ATPase with the c_8 ring. (*F*) The ground-state structure of bovine F_1-ATPase.

The most striking difference between the structures of the inactive *C. thermarum* wild-type and mutant states is that the most open of the three catalytic β-subunits, the β_E-subunit, is occupied by both an ADP molecule, with no associated magnesium ion, and by a phosphate ion bound in a position 7 Å from the γ-phosphate of a bound ATP molecule. A similar occupancy of ADP and phosphate in the β_E-subunit has never been observed in any of the many structures of states derived from an active F_1-ATPase, suggesting that it may be the basis of the mechanism of inhibition of ATP hydrolysis in *C. thermarum*. Following the hydrolysis of an ATP molecule in a closed catalytic site of F_1-ATPase, as the site opens in response to rotation of the γ-subunit driven by ATP hydrolysis in another catalytic site, the order of product release is not known, although it appears that the first product to leave as the catalytic site opens is the magnesium ion. However, there are conflicting data about whether ADP is released before phosphate or vice versa, although in other NTPases, ADP leaves last (46). Thus, one interpretation of the current information is that after ATP hydrolysis in the β_{DP}-site that subsequently becomes the observed β_E-site in the structure, the magnesium ion leaves followed by ADP, which then rebinds in a concentration-dependent manner. Another possibility is that the magnesium ion and phosphate leave after hydrolysis, and phosphate then rebinds in a concentration-dependent manner. The current structure favors the former mechanism. Thus, quantitative measurement of the affinities of ADP and phosphate and the structure of the enzyme artificially activated with LDAO would help to test these interpretations.

Knowledge of the mechanism of inhibition of the *C. thermarum* and other bacterial F-ATPases similarly inhibited in ATP hydrolysis could have practical benefits. For example, the F-ATPase from *Mycobacterium tuberculosis* is a validated drug target for treatment of tuberculosis, and knowledge of the mechanism of inhibition of ATP synthesis in this organism, and in other pathogenic bacteria, could provide new opportunities for drug development.

Materials and Methods

For purification and crystallization of bacterial F_1-ATPase, the *C. thermarum* F_1-ATPase (wild-type and mutant) was expressed from versions of plasmid

pTrc99A (47) with a His_{10} tag and a cleavage site for the tobacco etch virus (TEV) protease at the N terminus of subunit ε. The enzyme was purified by nickel affinity chromatography and cleaved on-column with TEV protease. Crystals grown by the microbatch method were cryocooled, and data were collected at the European Synchrotron Radiation Facility, Grenoble, France. For full details of these processes and of the structure determination and analysis, see *SI Materials and Methods*.

ACKNOWLEDGMENTS. We thank Dr. D. M. Rees for preparing *Escherichia coli* C41(Δ*unc*), and the beamline staff at the European Synchrotron Radiation Facility for their help. This work was supported by the Medical Research Council UK by Grants MC_U1065663150 (to J.E.W.) and MC_U105184325 (to A.G.W.L.), and by Programme Grant MR/M009858/1 (to J.E.W.). G.M.C. was supported by a James Cook Fellowship from the Royal Society of New Zealand and the Health Research Council of New Zealand.

1. Walker JE (2013) The ATP synthase: The understood, the uncertain and the unknown. *Biochem Soc Trans* 41(1):1–16.
2. Nalin CM, McCarty RE (1984) Role of a disulfide bond in the γ subunit in activation of the ATPase of chloroplast coupling factor 1. *J Biol Chem* 259(11):7275–7280.
3. Hisabori T, Konno H, Ichimura H, Strotmann H, Bald D (2002) Molecular devices of chloroplast F(1)-ATP synthase for the regulation. *Biochim Biophys Acta* 1555(1–3): 140–146.
4. Pullman ME, Monroy GC (1963) A naturally occuring inhibitor of mitochondrial adenosine triphosphatase. *J Biol Chem* 238(11):3762–3769.
5. Gledhill JR, Montgomery MG, Leslie AGW, Walker JE (2007) How the regulatory protein, IF(1), inhibits F(1)-ATPase from bovine mitochondria. *Proc Natl Acad Sci USA* 104(40):15671–15676.
6. Robinson GC, et al. (2013) The structure of F_1-ATPase from *Saccharomyces cerevisiae* inhibited by its regulatory protein IF_1. *Open Biol* 3(2):120164.
7. Bason JV, Montgomery MG, Leslie AGW, Walker JE (2014) Pathway of binding of the intrinsically disordered mitochondrial inhibitor protein to F_1-ATPase. *Proc Natl Acad Sci USA* 111(31):11305–11310.
8. Morales-Ríos E, et al. (2010) A novel 11-kDa inhibitory subunit in the F_1F_O ATP synthase of *Paracoccus denitrificans* and related α-proteobacteria. *FASEB J* 24(2):599–608.
9. Serrano P, Geralt M, Mohanty B, Wüthrich K (2014) NMR structures of α-proteobacterial ATPase-regulating ζ-subunits. *J Mol Biol* 426(14):2547–2553.
10. Morales-Rios E, Montgomery MG, Leslie AGW, Walker JE (2015) Structure of ATP synthase from *Paracoccus denitrificans* determined by X-ray crystallography at 4.0 Å resolution. *Proc Natl Acad Sci USA* 112(43):13231–13236.
11. Laget PP, Smith JB (1979) Inhibitory properties of endogenous subunit epsilon in the *Escherichia coli* F_1 ATPase. *Arch Biochem Biophys* 197(1):83–89.
12. Kato-Yamada Y, et al. (1999) ε subunit, an endogenous inhibitor of bacterial F(1)-ATPase, also inhibits F(0)F(1)-ATPase. *J Biol Chem* 274(48):33991–33994.
13. Yagi H, et al. (2009) Structural and functional analysis of the intrinsic inhibitor subunit ε of F_1-ATPase from photosynthetic organisms. *Biochem J* 425(1):85–94.
14. Wilkens S, Dahlquist FW, McIntosh LP, Donaldson LW, Capaldi RA (1995) Structural features of the ε subunit of the *Escherichia coli* ATP synthase determined by NMR spectroscopy. *Nat Struct Biol* 2(11):961–967.
15. Uhlin U, Cox GB, Guss JM (1997) Crystal structure of the ε subunit of the proton-translocating ATP synthase from *Escherichia coli*. *Structure* 5(9):1219–1230.
16. Wilkens S, Capaldi RA (1998) Solution structure of the ε subunit of the F_1-ATPase from *Escherichia coli* and interactions of this subunit with β subunits in the complex. *J Biol Chem* 273(41):26645–26651.
17. Yagi H, et al. (2007) Structures of the thermophilic F_1-ATPase ε subunit suggesting ATP-regulated arm motion of its C-terminal domain in F_1. *Proc Natl Acad Sci USA* 104(27):11233–11238.
18. Shirakihara Y, et al. (2015) Structure of a thermophilic F_1-ATPase inhibited by an ε-subunit: Deeper insight into the ε-inhibition mechanism. *FEBS J* 282(15):2895–2913.
19. Cingolani G, Duncan TM (2011) Structure of the ATP synthase catalytic complex (F(1)) from *Escherichia coli* in an autoinhibited conformation. *Nat Struct Mol Biol* 18(6): 701–707.
20. Shah NB, Hutcheon ML, Haarer BK, Duncan TM (2013) F_1-ATPase of *Escherichia coli*: The ε-inhibited state forms after ATP hydrolysis, is distinct from the ADP-inhibited state, and responds dynamically to catalytic site ligands. *J Biol Chem* 288(13): 9383–9395.
21. Shah NB, Duncan TM (2015) Aerobic growth of *Escherichia coli* is reduced and ATP synthesis is selectively inhibited when five C-terminal residues are deleted from the ε subunit of ATP synthase. *J Biol Chem* 290(34):21032–21041.
22. Taniguchi N, Suzuki T, Berney M, Yoshida M, Cook GM (2011) The regulatory C-terminal domain of subunit ε of F_oF_1 ATP synthase is dispensable for growth and survival of *Escherichia coli*. *J Bacteriol* 193(8):2046–2052.
23. Cook GM, et al. (2003) Purification and biochemical characterization of the F_1F_o-ATP synthase from thermoalkaliphilic *Bacillus* sp. strain TA2.A1. *J Bacteriol* 185(15): 4442–4449.
24. Nakagawa H, Lee SH, Kalra VK, Brodie AF (1977) Trypsin-induced changes in the orientation of latent ATPase in protoplast ghosts from *Mycobacterium phlei*. *J Biol Chem* 252(22):8229–8234.
25. Haagsma AC, Driessen NN, Hahn MM, Lill H, Bald D (2010) ATP synthase in slow- and fast-growing mycobacteria is active in ATP synthesis and blocked in ATP hydrolysis direction. *FEMS Microbiol Lett* 313(1):68–74.
26. Hoffmann A, Dimroth P (1990) The ATPase of *Bacillus alcalophilus*. Purification and properties of the enzyme. *Eur J Biochem* 194(2):423–430.
27. Hicks DB, Krulwich TA (1990) Purification and reconstitution of the F_1F_0-ATP synthase from alkaliphilic *Bacillus firmus* OF4. Evidence that the enzyme translocates H^+ but not Na^+. *J Biol Chem* 265(33):20547–20554.
28. Stocker A, Keis S, Vonck J, Cook GM, Dimroth P (2007) The structural basis for unidirectional rotation of thermoalkaliphilic F_1-ATPase. *Structure* 15(8):904–914.
29. Kato S, Yoshida M, Kato-Yamada Y (2007) Role of the ε subunit of thermophilic F_1-ATPase as a sensor for ATP. *J Biol Chem* 282(52):37618–37623.
30. Gibbons C, Montgomery MG, Leslie AGW, Walker JE (2000) The structure of the central stalk in bovine F(1)-ATPase at 2.4 Å resolution. *Nat Struct Biol* 7(11): 1055–1061.
31. Gledhill JR, Montgomery MG, Leslie AGW, Walker JE (2007) Mechanism of inhibition of bovine F_1-ATPase by resveratrol and related polyphenols. *Proc Natl Acad Sci USA* 104(34):13632–13637.
32. Bowler MW, Montgomery MG, Leslie AGW, Walker JE (2006) How azide inhibits ATP hydrolysis by the F-ATPases. *Proc Natl Acad Sci USA* 103(23):8646–8649.
33. Rees DM, Montgomery MG, Leslie AGW, Walker JE (2012) Structural evidence of a new catalytic intermediate in the pathway of ATP hydrolysis by F_1-ATPase from bovine heart mitochondria. *Proc Natl Acad Sci USA* 109(28):11139–11143.
34. Bason JV, Montgomery MG, Leslie AGW, Walker JE (2015) How release of phosphate from mammalian F_1-ATPase generates a rotary substep. *Proc Natl Acad Sci USA* 112(19):6009–6014.
35. Lu S, et al. (2014) The structural basis of ATP as an allosteric modulator. *PLoS Comput Biol* 10(9):e1003831.
36. Kabaleeswaran V, Puri N, Walker JE, Leslie AGW, Mueller DM (2006) Novel features of the rotary catalytic mechanism revealed in the structure of yeast F_1 ATPase. *EMBO J* 25(22):5433–5442.
37. Watt IN, Montgomery MG, Runswick MJ, Leslie AGW, Walker JE (2010) Bioenergetic cost of making an adenosine triphosphate molecule in animal mitochondria. *Proc Natl Acad Sci USA* 107(39):16823–16827.
38. Bowler MW, Montgomery MG, Leslie AGW, Walker JE (2007) Ground state structure of F_1-ATPase from bovine heart mitochondria at 1.9 Å resolution. *J Biol Chem* 282(19): 14238–14242.
39. Kabaleeswaran V, et al. (2009) Asymmetric structure of the yeast F_1 ATPase in the absence of bound nucleotides. *J Biol Chem* 284(16):10546–10551.
40. Suzuki T, et al. (2003) F_0F_1-ATPase/synthase is geared to the synthesis mode by conformational rearrangement of ε subunit in response to proton motive force and ADP/ATP balance. *J Biol Chem* 278(47):46840–46846.
41. Keis S, Stocker A, Dimroth P, Cook GM (2006) Inhibition of ATP hydrolysis by thermoalkaliphilic F_1F_o-ATP synthase is controlled by the C terminus of the epsilon subunit. *J Bacteriol* 188(11):3796–3804.
42. Jault JM, et al. (1995) The $\alpha_3\beta_3\gamma$ complex of the F_1-ATPase from thermophilic *Bacillus* PS3 containing the $\alpha D_{261}N$ substitution fails to dissociate inhibitory MgADP from a catalytic site when ATP binds to noncatalytic sites. *Biochemistry* 34(50):16412–16418.
43. Nakanishi-Matsui M, et al. (2006) Stochastic high-speed rotation of *Escherichia coli* ATP synthase F_1 sector: The epsilon subunit-sensitive rotation. *J Biol Chem* 281(7): 4126–4131.
44. Lötscher HR, deJong C, Capaldi RA (1984) Interconversion of high and low adenosinetriphosphatase activity forms of *Escherichia coli* F_1 by the detergent lauryldimethylamine oxide. *Biochemistry* 23(18):4140–4143.
45. Dunn SD, Tozer RG, Zadorozny VD (1990) Activation of *Escherichia coli* F_1-ATPase by lauryldimethylamine oxide and ethylene glycol: Relationship of ATPase activity to the interaction of the ε and β subunits. *Biochemistry* 29(18):4335–4340.
46. Nitta R, Okada Y, Hirokawa N (2008) Structural model for strain-dependent microtubule activation of Mg-ADP release from kinesin. *Nat Struct Mol Biol* 15(10): 1067–1075.
47. Stocker A, Keis S, Cook GM, Dimroth P (2005) Purification, crystallization, and properties of F_1-ATPase complexes from the thermoalkaliphilic *Bacillus* sp. strain TA2.A1. *J Struct Biol* 152(2):140–145.
48. Leslie AGW (2006) The integration of macromolecular diffraction data. *Acta Crystallogr D Biol Crystallogr* 62(Pt 1):48–57.
49. Battye TG, Kontogiannis L, Johnson O, Powell HR, Leslie AG (2011) iMOSFLM: A new graphical interface for diffraction-image processing with MOSFLM. *Acta Crystallogr D Biol Crystallogr* 67(Pt 4):271–281.
50. Evans P (2006) Scaling and assessment of data quality. *Acta Crystallogr D Biol Crystallogr* 62(Pt 1):72–82.
51. French G, Wilson K (1978) On the treatment of negative intensity observations. *Acta Crystallogr A* 34:517–525.
52. McCoy AJ, et al. (2007) Phaser crystallographic software. *J Appl Crystallogr* 40(Pt 4): 658–674.
53. Murshudov GN, et al. (2011) REFMAC5 for the refinement of macromolecular crystal structures. *Acta Crystallogr D Biol Crystallogr* 67(Pt 4):355–367.
54. Emsley P, Lohkamp B, Scott WG, Cowtan K (2010) Features and development of Coot. *Acta Crystallogr D Biol Crystallogr* 66(Pt 4):486–501.
55. Chen VB, et al. (2010) MolProbity: All-atom structure validation for macromolecular crystallography. *Acta Crystallogr D Biol Crystallogr* 66(Pt 1):12–21.
56. Schrodinger LLC (2015) The PyMOL Molecular Graphics System, Version 1.8. Available at pymol.org. Accessed August 31, 2016.